LOCKED RIGID ORIGAMI WITH MULTIPLE DEGREES OF FREEDOM

ZACHARY ABEL, THOMAS C. HULL, AND TOMOHIRO TACHI

1. Introduction

Many practical applications of origami involve folding hard or thick material such as metal and cardboard sheets. Such situations are well-modeled as rigid origami, i.e., a model based on rigid panels and hinges which forbids both the material bending and traveling creases. The continuous foldability of rigid origami from a flat unfolded state to the folded state is essential for enabling folding-based manufacturing processes to make various 3D forms and tessellations.

Many origami models are not rigidly foldable from the unfolded state because they contain a "locked" state which cannot be unfolded without bending the material. We tend to explain such a lock as being attributed to the collision of facets or the lack of degrees of freedom. In fact, many locked rigid origami models can be continuously unfolded in kinematic simulations if the crease pattern, which is a polygonal mesh, is triangulated to have multiple degrees of freedom. This observation leads to a hypothesis that any triangulated mesh origami can be continuously folded from an unfolded state. However, in this paper we show that a triangulated crease pattern is not enough to make it rigid-foldable by constructing a locked rigid origami model from a triangulated crease pattern. The proposed rigid origami model is a developable triangular mesh with 6 boundary edges (thus with 3 degrees of freedom) and yet has a folded state which cannot be continuously unfolded to a flat sheet of paper even if faces are allowed to penetrate each other (as explained at the end of Section 3).

We investigate the full three-dimensional configuration space of the proposed model and prove that the configuration space is comprised of two disconnected domains. We further parameterize the pattern by a sector angle θ and explore its family to find out the critical patterns at which the configuration space changes its topology.

2. Description of the model

The crease pattern of the origami model can be seen in Figure 1, left, where the bold lines are mountain creases and the dashed lines are valleys. There is a small valley-folded equilateral in the center and a larger mountain-folded equilateral triangle surrounding it. The vertices of the valley triangle meet the edges of the mountain triangle at the 2/3 point along the mountain edges.

1991 *Mathematics Subject Classification.* Primary 52C25, 53C24; Secondary 70B10.
Key words and phrases. folding, rigidity, rigid origami.

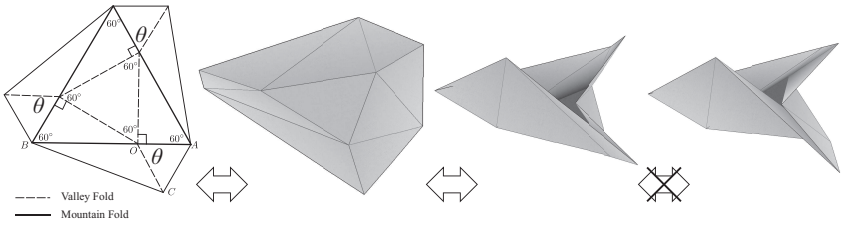

FIGURE 1. The crease pattern (left), continuous folding (middle two), and locked folded states (right) of the proposed pattern. Red and blue lines indicate mountain and valley creases respectively. θ is the parameter that changes the connectivity of the configuration space; in this figure θ is set to 62°

This crease pattern is based on the triangle twist (see [Fujmoto and Nishiwaki 82] or [Gjerde 08]); if we take $\theta = 60°$ and the short, mountain creases that are perpendicular to the valley equilateral triangle are removed (like OA), then this is exactly a triangle twist. Triangle twists with this mountain-valley assignment do not fold rigidly (the reasoning is the same as for square twists with similar mountain-valley assignments; see [Hull 13]), but with the addition of the short mountain creases OA and its symmetric counterparts, the crease pattern will fold rigidly into a three-dimensional shape, as seen in the middle two images of Figure 1.

We claim that for $60° < \theta < 66.715°$ this origami model will have a *locked state*, by which we mean a folded state where the three degrees of freedom cannot be continuously changed to rigidly unfold the model to the flat, unfolded state. Here, a continuous rigid folding/unfolding motion in our model allows for self-penetration, but not for *facet flipping*. A facet flip occurs when a fold angle of a crease becomes $\pm\pi$ and jumps to $\mp\pi$. We avoid such a motion so that the continuous transformation is a discrete (piecewise isometric) version of a homotopy of two states. The rightmost images in Figure 1 are meant to illustrate a locked state for the model where $\theta = 62°$.

3. Proof of the locked state

To prove that this model has a locked rigidly-folded state, we need to analyze the rigid motions of the faces. Figure 2 shows the two nested triangles in the crease pattern and how we situate it in the xy-plane. Think of this as embedded in $\mathbb{R}^3$ so that we can fold it into a three-dimensional shape. The point O is the origin.

Our aim is to find equations that govern how the folding angles (which equal $\pi-$ the dihedral angles) labeled α, β, and γ interact as we fold the model rigidly. Since the crease with folding angle α lies on the positive y-axis, the point A will swing along a circle as α increases (from an unfolded angle of 0° up to possible a flat-folded angle of 180°). Thus the position of A as this model is folded will be

$$\overrightarrow{OA} = (\cos\alpha, 0, \sin\alpha).$$

The motion of point B will be similar, except governed by folding angle β and in a different position. We can find its position by rotating the vector $\overrightarrow{OA}$ by $-120°$

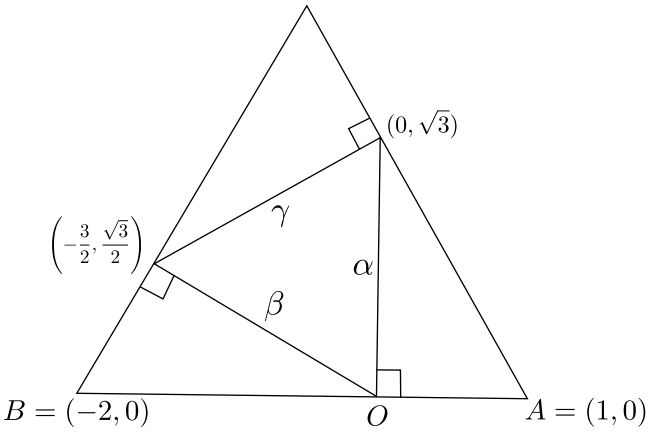

FIGURE 2. Setting the crease pattern in the xy-plane. O is the origin and the z-axis is in your face.

and translating by $(-3/2, \sqrt{3}/2, 0)$. Thus

$$\overrightarrow{OB} = \begin{pmatrix} -\frac{1}{2} & \frac{\sqrt{3}}{2} & 0 \\ -\frac{\sqrt{3}}{2} & -\frac{1}{2} & 0 \\ 0 & 0 & 1 \end{pmatrix} \begin{pmatrix} \cos\beta \\ 0 \\ \sin\beta \end{pmatrix} + \begin{pmatrix} -\frac{3}{2} \\ \frac{\sqrt{3}}{2} \\ 0 \end{pmatrix}$$

$$= (-\frac{1}{2}\cos\beta - \frac{3}{2}, -\frac{\sqrt{3}}{2}\cos\beta + \frac{\sqrt{3}}{2}, \sin\beta).$$

Now, referring to the crease pattern in Figure 1 again, we can see that as the inner triangle of valley creases folds, whether or not $\triangle OAC$ and $\triangle OBC$ intersect can be determined by the angle between the vectors $\overrightarrow{OA}$ and $\overrightarrow{OB}$ as they fold. Now, $\angle AOC = \theta$ and $\angle COB = 180° - \theta$. The triangles in question will lie in the same plane if and only if the angle between $\overrightarrow{OA}$ and $\overrightarrow{OB}$ in a folded state is $180° - 2\theta$. This angle cannot be less that $180° - 2\theta$; it represents the smallest angle that can be between $\overrightarrow{OA}$ and $\overrightarrow{OB}$ or else the paper would have to rip, say along OC. A good way to check this is to use the dot product of $\overrightarrow{OA}$ and $\overrightarrow{OB}$, which will equal $2\cos\rho$ where ρ is the angle between the vectors. (Note from Figure 2 that $|OA| = 1$ and $|OB| = 2$.)

Thus we obtain

$$-\frac{1}{2}\cos\alpha\cos\beta - \frac{3}{2}\cos\alpha + \sin\alpha\sin\beta = 2\cos\rho \leq 2\cos(180° - 2\theta). \tag{1}$$

The reason for the direction of the inequality is because vectors $\overrightarrow{OA}$ and $\overrightarrow{OB}$ start at 180° from each other in the unfolded state, so then the dot product will be -2. As the model folds this dot product will increase until the angle reached between these two vectors is $180° - 2\theta$, after which the angle cannot get any smaller. So keeping the dot product $\leq 2\cos(180° - 2\theta)$ is desired.

Of course, we can do this with all pairs of the folding angles about the valley-folded inner triangle:

$$-\frac{1}{2}\cos\beta\cos\gamma - \frac{3}{2}\cos\beta + \sin\beta\sin\gamma \leq 2\cos(180° - 2\theta) \tag{2}$$

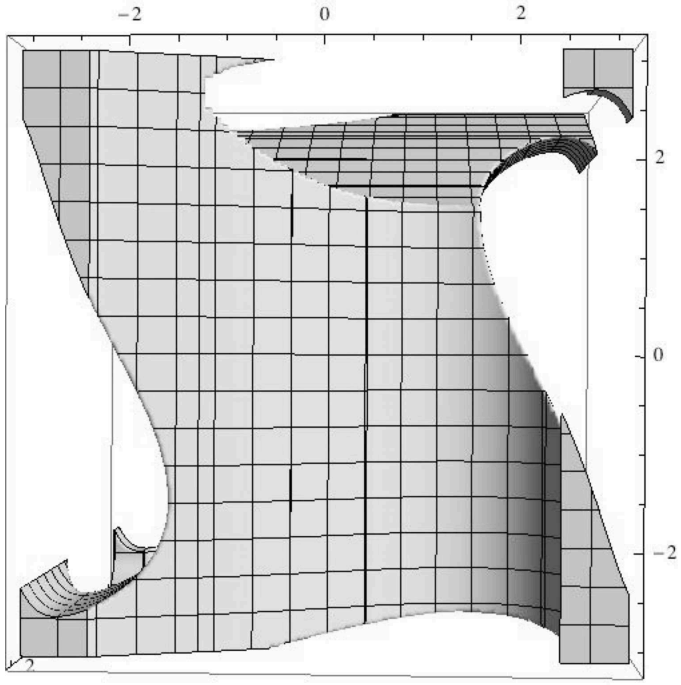

FIGURE 3. The configuration space of points (α, β, γ) that satisfy the dot product inequalities, where $\theta = 62°$.

$$-\frac{1}{2}\cos\gamma\cos\alpha - \frac{3}{2}\cos\gamma + \sin\gamma\sin\alpha \leq 2\cos(180° - 2\theta) \tag{3}$$

Plotting the region of triples (α, β, γ) that satisfy all these equations gives the picture in Figure 3, where $-\pi \leq \alpha, \beta, \gamma \leq \pi$ and we take $\theta = 62°$. Notice that the space appears disconnected. The isolated corner where the folding angles α, β, and γ are all close to π (and thus the inner valley triangle is close to being folded flat) will be a locked state of our folded crease pattern, with no way to rigidly unfold to the flat paper state.

We need to prove, however, that this configuration space (in the range $[-\pi, \pi]$ and with $\theta = 62°$) is disconnected. To do this, fix one of the folding angles, say γ, to be $2\pi/3$ and let the other two have values $2\pi/3 \leq \alpha, \beta \leq \pi$. If we graph the left-hand side of one of the inequalities (either the α, γ one or the β, γ one) along with the constant function $y = 2\cos 56°$ (since $180° - 2 \cdot 62° = 56°$), then we can see that the expression is clearly greater than $2\cos 56°$ (see Figure 4). Thus the α, γ inequalities will not hold when $\gamma = 2\pi/3$ and $2\pi/3 \leq \alpha \leq \pi$. Since the equations are exactly the same, we also get that the inequalities will not hold when $\gamma = 2\pi/3$ and $2\pi/3 \leq \beta \leq \pi$. This means that the square $2\pi/3 \leq \alpha, \beta \leq \pi$ when $\gamma = 2\pi/3$ is a region in $\mathbb{R}^3$ where the inequalities do not hold.

Similarly, the squares $2\pi/3 \leq \ \beta, \gamma \leq \pi$ when $\alpha = 2\pi/3$ and $2\pi/3 \leq \alpha, \gamma \leq \pi$ when $\beta = 2\pi/3$ are regions where the inequalities do not hold. These three squares in $\mathbb{R}^3$ isolate the corner of the configuration space seen in Figure 3 around the point (π, π, π), proving that this section is disconnected from the main part of the

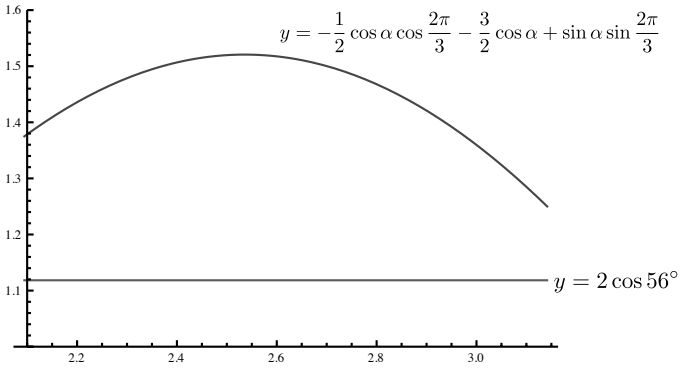

FIGURE 4. Comparing the left-hand side of an inequality with $y = 2\cos 56^\circ$ when $\gamma = 2\pi/3$.

configuration space. In other words, we cannot rigidly unfold from this corner near (π, π, π) to the unfolded state, which is the point $(0, 0, 0)$.

The dot product we use in this model also describes what is going wrong with the folded paper to make the configuration space disconnected. Since inequality (1) amounts to

$$\overrightarrow{OA} \cdot \overrightarrow{OB} = 2\cos\rho \leq \cos(180^\circ - 2\theta)$$

where ρ is the angle between the vectors $\overrightarrow{OA}$ and $\overrightarrow{OB}$, and $180^\circ - 2\theta$ is the smallest ρ can be, we have that *the folded paper fails to be rigid because* $\overrightarrow{OA}$ *and* $\overrightarrow{OB}$ *are too close together*, not necessarily because the paper is penetrating itself, for instance. This is quite counterintuitive; examining a physical model and simulations like that shown in Figure 1 make it seem that the paper is trying to self-intersect. The failure of our inequalities (1), (2), and (3) is not caused by self-intersection of the paper.

4. The critical value of θ

Examination of the configuration space for different values of θ reveals the existence of a critical value of θ where the space becomes disconnected along the line $\alpha = \beta = \gamma$. This is shown in Figure 5, where this critical value seems to be in the range $66.5^\circ < \theta < 67^\circ$. Note that in the $\theta = 67^\circ$ image in Figure 5 there are

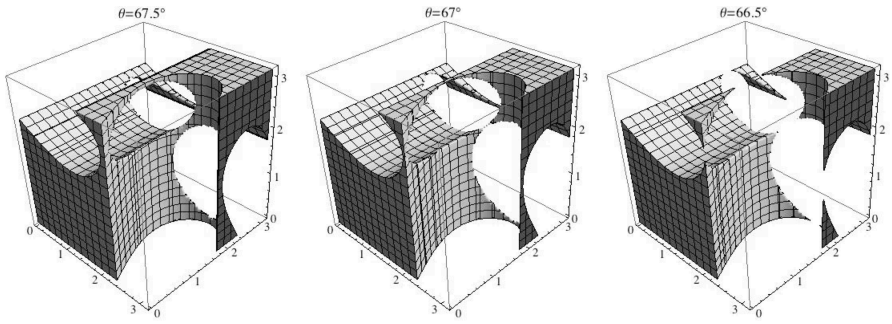

FIGURE 5. Details of the configuration space for three values of θ showing how the disconnection emerges.

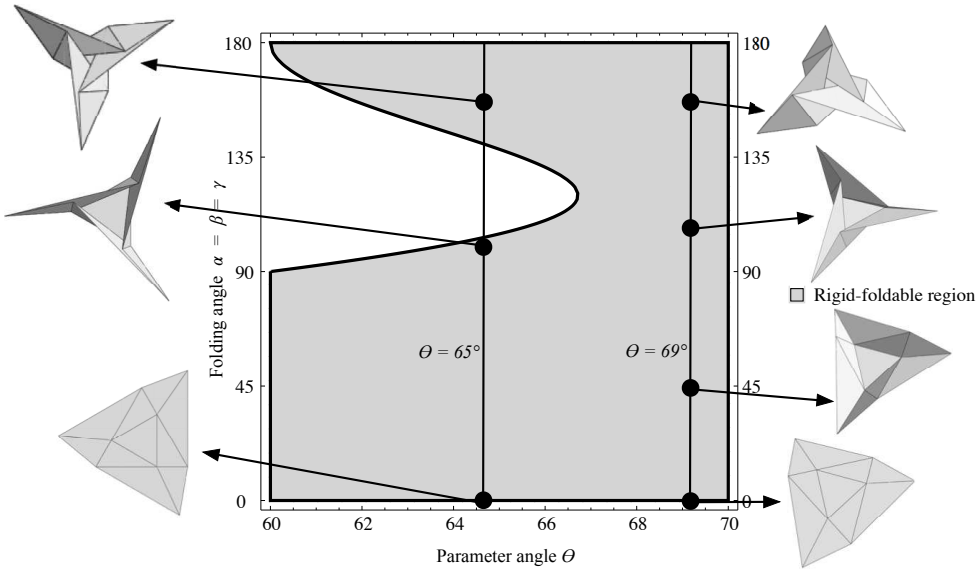

FIGURE 6. A parameter space plot where we let $\alpha = \beta = \gamma$ be the vertical axis and θ be the horizontal axis.

"bridges" when one of the folding angles equals π connecting the main configuration space to the soon-to-be-disconnected portion where one of the angles α, β, or γ equals π. However, these bridges do not exist as such a motion requires a facet flip where the fold angle of the crease OA passes $\pm\pi$. This cannot happen not only in reality because of self-collision, but also in our model allowing for self-intersection. We conclude that the bridges are merely artifacts of the dot product inequalities (1)-(3) and not actually part of the configuration space. (See Section 5 for more evidence of this.)

The critical value for θ along this diagonal of the configuration space can be computed by letting $\alpha = \beta = \gamma$ in our dot product inequality and noticing that the left-hand side becomes a quadratic in $\cos\alpha$:

$$-\frac{3}{2}(\cos\alpha + \frac{1}{2})^2 + \frac{11}{8} \leq 2\cos(180^\circ - 2\theta). \tag{4}$$

The left side of (4) reaches its maximum of $11/8$ at $\alpha = 120^\circ$, and the right-hand side will equal this when

$$\theta = \frac{1}{2}\arccos(-\frac{11}{16}) \approx 66.7163^\circ.$$

Another way to see the critical value emergence is to plot values of θ with the dot product inequality with $\alpha = \beta = \gamma$. The inequality will define a region where rigid folding is allowed, and each vertical line in this plot will illustrate if the folding angles can be made from 0 to 180 degrees with the our inequalities remaining valid. This is shown in Figure 6. This plot verifies that the range of θ where a locked state exists in the model is from $\theta = 60^\circ$ to approximately $\theta = 66.716^\circ$. Also notice that the boundary between the locked state region and the rigidly foldable region approximates a quadratic curve near the critical value.

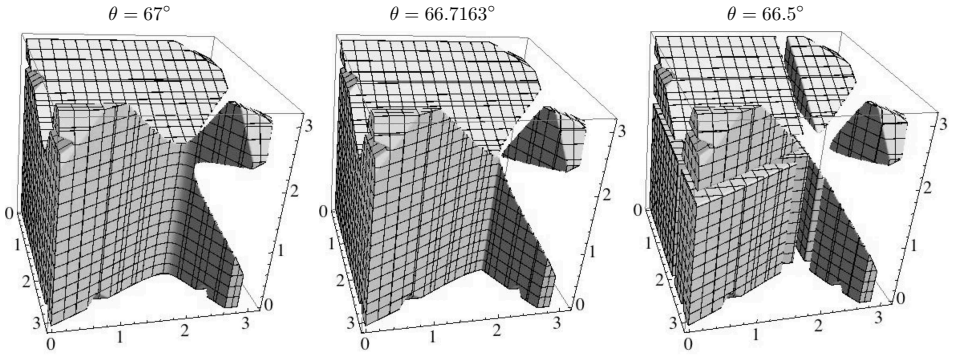

FIGURE 7. The configuration space for self-intersections where the axes are the folding angles α, β, and γ, taken at three values of θ near the critical value $\theta = 66.7163°$.

5. Configuration space for self-intersections

Since the dot product model captured in the inequalities (1)-(3) only addresses one type of rigidity failure (where certain crease lines move too close together), it is natural to seek a way to capture the failure of rigidity by way of the paper intersecting itself. This can be done by making a kinematic model of the folding paper, which is based on rotations in $\mathbb{R}^3$ done in sequence to model the multiple creases folding simultaneously. (See [Balkcom and Mason 08] for details.) This model was implemented in Mathematica; the code can be downloaded at this web page: `http://mars.wne.edu/~thull/trimesh/mesh.html`

Once we have this kinematic model, we can detect facet flips as follows: During the folding consider the vector $\overrightarrow{OA}$ (see Figure 1) and the vector $\overrightarrow{n} = \overrightarrow{OB} \times \overrightarrow{OC}$ which is normal to the OBC plane. When the paper first folds from a flat state, $\overrightarrow{OA}$ and $\overrightarrow{n}$ will form an acute angle to one another, making their dot product non-negative. If $\overrightarrow{OA} \cdot \overrightarrow{n} < 0$ then $\overrightarrow{OA}$ will have passed through the OBC plane and caused a facet flip. Checking this condition with the similar creases at the other two vertices gives us the configuration spaces shown in Figure 7, where we've taken different values of θ near the critical value $\theta = 66.7163°$.

We notice a few things: (1) That facet flipping seems to be happening around the same critical value for θ as for the creases OA and OC getting too close together. This makes sense because these creases seem to get too close to each other only after OA folds onto the OBC plane. (2) The "bridges" from the configuration spaces in Figures 3 and 5 are absent from the non-facet flipping configuration space, confirming our previous claim that those bridges are not actually foldable configurations.

6. Conclusion

We have created a triangular crease pattern (mesh) that can be put into a three-dimensional locked state, where attempts to unfold from such a state would cause rigidity of the triangles in the mesh to fail. This proves that it is possible to have a triangulated crease pattern that does not allow full rigid folding in the model's configuration space. In other words, triangulating a non-rigidly-foldable crease pattern

is not always enough to attain a rigid folding. By changing one angle parameter, we can control the gap between two separate configuration spaces. In real elastic material, such a gap yields a snap-through effect, possibly leading to engineering applications with multi-stable structures. (For example, see [Silverberg et al. 15].)

Of course, this is only one example, and other such triangle meshes with locked, rigid states must exist. Nonetheless, our example has a number of parameters one could adjust to meet design constraints (like the shape of the boundary or modifying the other angles in the crease pattern). Also, it would be very interesting to find a way to tessellate this crease pattern, which might be possible since the triangle twist, on which our example is based, tessellates easily (see [Gjerde 08]). However, our changing of the angle θ to be greater than $60°$, so as to make a truly three-dimensional locked model, prohibits the obvious method of tessellating that one would try, and we have not yet found an alternate solution.

Acknowledgments

This work began at the 2013 Bellairs Workshop on Computational Geometry, co-organized by Erik Demaine and Godfried Toussaint. We thank the other participants of the workshop for helpful discussions.

Research by Z. Abel supported by NSF Graduate Fellowship, NSF ODISSEI grant EFRI-1240383, and NSF Expedition grant CCF-1138967. Research of T. Hull supported by NSF grant EFRI-ODISSEI-1240441 "Mechanical Meta-Materials from Self-Folding Polymer Sheets". Research of T. Tachi supported by the Japan Science and Technology Agency Presto program.

References

[Balkcom and Mason 08] Devin J. Balkcom and Matthew T. Mason. "Robotic Origami Folding." *International Journal of Robotics Research* 27:5 (2008), 613–627.

[Fujmoto and Nishiwaki 82] Shuzo Fujmoto and Masami Nishiwaki. *Sozo suru origami asobi e no shotai (Invitation to Playing with Creative Origami, Japanese)*. Tokyo: Asahi Culture Center, 1982.

[Gjerde 08] Eric Gjerde. *Origami Tessellations: Are-Inspiring Geometric Designs*. Wellesley, MA: A K Peters/CRC Press, 2008.

[Hull 13] Thomas C. Hull. *Project Origami: Activities for Exploring Mathematics*, Second edition. Wellesley, MA: A K Peters/CRC Press, 2013.

[Silverberg et al. 15] Jessie L. Silverberg, Jun-Hee Na, Arthur A. Evans, Bin Liu, Thomas C. Hull, Christian D. Santangelo, Robert J. Lang, Ryan C. Hayward, and Itai Cohen. "Origami structures with a critical transition to bistability arising from hidden degrees of freedom." *Nature Materials*. 3/09/15 advance online publication.

Abel: CSAIL, MIT, Cambridge MA, USA
E-mail address: zabel@mit.edu

Hull: Department of Mathematics, Western New England University, Springfield MA, USA
E-mail address: thull@wne.edu

Tachi: Department of General Systems Studies, The University of Tokyo, Japan
E-mail address: tachi@idea.c.u-tokyo.acjp